Journal of Solid State Chemistry 181 (2008) 3189–3193

Contents lists available at ScienceDirect

Journal of Solid State Chemistry

journal homepage: www.elsevier.com/locate/jssc

Syntheses, structures, and magnetic and optical properties of the compounds $[Hg_3Te_2][UCl_6]$ and $[Hg_4As_2][UCl_6]$

Daniel E. Bugaris, James A. Ibers *

Department of Chemistry, Northwestern University, 2145 Sheridan Road, Evanston, IL 60208-3113, USA

ARTICLE INFO

Article history:
Received 1 May 2008
Received in revised form
7 August 2008
Accepted 11 August 2008
Available online 22 August 2008

Keywords:
Uranium mercury chalcogenide
Uranium mercury pnictide
$[UCl_6]^{2-}$
Crystal structures
Syntheses

ABSTRACT

Two new quaternary salts, $[Hg_3Te_2][UCl_6]$ and $[Hg_4As_2][UCl_6]$, have been synthesized and their structures determined by single-crystal X-ray diffraction analysis. $[Hg_3Te_2][UCl_6]$ is the product of a reaction involving UCl_4, $HgCl_2$, and HgTe at 873 K. The compound crystallizes in space group $P2_1/c$ of the monoclinic system. $[Hg_4As_2][UCl_6]$ results from the reaction of U, Hg_2Cl_2, and As at 788 K. It crystallizes in space group *Pbca* of the orthorhombic system. $[Hg_3Te_2][UCl_6]$ has a two-dimensional framework of $^2_\infty[Hg_3Te_2^{2+}]$ layers, whereas $[Hg_4As_2][UCl_6]$ has a three-dimensional framework of $^2_\infty[Hg_3As_2]$ layers interconnected by Hg atoms linearly bonded to As atoms. Both framework structures contain discrete $[UCl_6]^{2-}$ anions between the layers. $[Hg_3Te_2][UCl_6]$ exhibits temperature-independent paramagnetism. The optical absorption spectra of these compounds display *f–f* transitions.

1. Introduction

The vast majority of uranium transition-metal chalcogenides (S, Se, or Te) or pnictides (P, As, Sb, or Bi) whose structures are known incorporate 3*d* or 4*d* transition metals. The few with 5*d* transition metals that have been studied by single-crystal X-ray diffraction methods include $Cs_8Hf_5UTe_{30.6}$ [1], $Ir_2U_6Se_{15.5}$ [2], HfU_3Sb_5 [3], and $AuUSb_2$ [4]. To probe 5*d*/5*f* systems, we have chosen the Hg/U system for which the binary phase diagram [5] reveals only the phases $Hg_{45}U_{11}$, Hg_3U, Hg_2U, and HgU. We have probed this system with the use of mercury halides as reagents. These reagents have been shown to react with metals and chalcogens or pnictogens to produce quaternary compounds, most of which are nothing more than salts but most of which have been described as "supramolecular compounds". The chemistry of such compounds is rich and includes $[Hg_3Q_2][SiF_6]$ (Q = S, Se, Te) [6], $[Hg_3Q_2][MX_6]$ (Q = S, Se; M = Zr, Hf; X = Cl, Br) [7], $[Hg_3Se_2][Se_2O_5]$ [8], $[Hg_6T_4][MX_6]X$ (T = P, As; M = Mo, Ti; X = Cl, Br) [9,10], $[Hg_7As_4][AgI_3]_2$ [11], $[Hg_3T_2][TlX_3]$ (T = As, Sb; X = Cl, Br) [12], $[Hg_6As_4][YbBr_6]Br$ [13], $[Hg_{11}As_4][GaBr_4]_4$ [14], and $[Hg_2As]_2[CdI_4]$ [15]. Here we report the syntheses, crystal structures, optical properties, and magnetic properties of the first Hg/U chalcogenides or pnictides, namely $[Hg_3Te_2][UCl_6]$ and $[Hg_4As_2][UCl_6]$.

2. Experimental

2.1. Syntheses

CCl_4 was dried over KH and distilled. UCl_4 was prepared by a modification of the literature procedure [16]. A 6.02 g (21.0 mmol) portion of UO_3 (Kerr-McGee Nuclear Corp.) was combined with 14.85 mL (105.3 mmol) of hexachloropropene (Aldrich, 96%) in a 150 mL round-bottom flask. The flask was fit with a condenser and placed under an N_2 atmosphere that was vented through a KOH bubbler. The N_2 had been passed over BASF catalyst at 353 K and then over Drierite to remove O_2 and H_2O. The flask was gradually heated to 403 K. This initiated an exothermic reaction that turned the solution into a deep-red color and released Cl_2 gas. Once the reaction was complete, the reaction mixture was allowed to reflux at 431 K for 3.5 h. The resulting green UCl_4 was separated from the solution by filtration through a cannula. Three successive washes of the product with 10 mL portions of CCl_4 were carried out. Residual CCl_4 was removed under vacuum.

Finely divided uranium powder was prepared by a modification of the literature procedure [17]. Uranium metal turnings (depleted, Oak Ridge National Laboratory) were washed with concentrated HNO_3 to remove any uranium oxide coating. The turnings were then rinsed with de-ionized water and dried with acetone. The uranium metal turnings were placed in a Schlenk vessel and reacted with an atmosphere of H_2 at 723 K to produce UH_3. UH_3 was converted to finely divided U powder under vacuum at 773 K.

* Corresponding author.
E-mail address: ibers@chem.northwestern.edu (J.A. Ibers).

0022-4596/$ - see front matter © 2008 Elsevier Inc. All rights reserved.
doi:10.1016/j.jssc.2008.08.019

The remaining reactants were used as obtained. Reactions were carried out in fused-silica tubes. The tubes were charged with reaction mixtures under an Ar atmosphere in a glove box and then they were evacuated to $\sim 10^{-4}$ Torr and flame sealed. Selected single crystals from each reaction were examined with an EDX-equipped Hitachi S-3400 SEM. The compounds are both moderately stable in air.

2.2. Synthesis of $[Hg_3Te_2][UCl_6]$

The reaction mixture consisted of UCl_4 (0.11 mmol), HgTe (0.22 mmol; Aldrich Chemical Co.), and $HgCl_2$ (0.11 mmol; Mallinckrodt, Inc.). The reaction mixture was heated to 1123 K in 24 h, kept at 1123 K for 96 h, cooled at 6.8 K/h to 473 K, and then cooled rapidly to 293 K. Green plates of $[Hg_3Te_2][UCl_6]$ in about 70% yield were the major product, and green needles of UCl_4 were the minor product. In an alternative heating procedure, the reaction mixture was heated to 873 K in 15 h, kept at 873 K for 120 h, and then the furnace was turned off. This synthesis produced larger crystals of $[Hg_3Te_2][UCl_6]$ suitable for further measurements. EDX analysis of the green crystals showed the presence of Hg, Te, U, and Cl.

2.3. Synthesis of $[Hg_4As_2][UCl_6]$

We have prepared single crystals of $[Hg_4As_2][UCl_6]$ by the reaction of U (0.13 mmol), Hg_2Cl_2 (0.38 mmol; Alfa), and As (0.51 mmol; Strem Chemicals, Inc., 2N). The sample was heated to 788 K in 12 h, kept at 788 K for 144 h, and then the furnace was turned off. The product consisted of red blocks of $[Hg_4As_2][UCl_6]$ in about 80% yield. EDX analysis of the crystals showed the presence of Hg, As, U, and Cl.

2.4. Structure determinations

Single-crystal X-ray diffraction data were collected with the use of graphite-monochromatized Mo$K\alpha$ radiation ($\lambda = 0.71073$ Å) at 153 K on a Bruker Smart-1000 CCD diffractometer [18]. The crystal-to-detector distance was 5.023 cm. Crystal decay was monitored by recollecting 50 initial frames at the end of the data collection. Data were collected by a scan of 0.3° in ω in groups of 606 frames at φ settings of 0°, 90°, 180°, and 270°. The exposure times for $[Hg_3Te_2][UCl_6]$ and $[Hg_4As_2][UCl_6]$ were 30 and 25 s/frame, respectively. The collection of intensity data was carried out with the program SMART [18]. Cell refinement and data reduction were carried out with the use of the program APEX2 [19]. A Leitz microscope equipped with a calibrated traveling micrometer eyepiece was employed to measure accurately the crystal dimensions; face-indexed absorption corrections were performed numerically with the use of the program XPREP [20]. Then the program SADABS [18] was employed to make incident beam and decay corrections. The structures were solved with the direct methods program SHELXS and refined with the full-matrix least-squares program SHELXL [20]. Each final refinement included anisotropic displacement parameters. The program STRUCTURE TIDY [21] was used to standardize the positional parameters. Additional experimental details are given in Table 1 and the Supporting material. Selected metrical details are presented in Tables 2 and 3.

2.5. Magnetic susceptibility measurement

DC magnetic measurements of $[Hg_3Te_2][UCl_6]$ were carried out with the use of a Quantum Design MPMS5 SQUID magnetometer. Twenty-seven milligrams of ground single crystals were loaded into a gelatin capsule. Both zero-field cooled (ZFC) and field-cooled (FC) measurements were made between 2 and 400 K with a measuring field of 500 G. All data were corrected for electron core diamagnetism [22].

Table 1
Crystal data and structure refinements for $[Hg_3Te_2][UCl_6]$ and $[Hg_4As_2][UCl_6]$[a]

	$[Hg_3Te_2][UCl_6]$	$[Hg_4As_2][UCl_6]$
Fw	1307.70	1402.93
Space group	$P2_1/c$	$Pbca$
Z	2	8
a (Å)	6.835(1)	13.316(1)
b (Å)	7.864(1)	13.636(1)
c (Å)	13.632(2)	16.853(2)
β (°)	91.530(2)	90
V (Å^3)	732.4(2)	3060.0(5)
ρ_c (g/cm^3)	5.929	6.090
μ (cm^{-1})	473.2	558.5
$R(F)$[b]	0.038	0.033
R_w (F^2)[c]	0.109	0.083

[a] For both structures, $T = 153(2)$ K and $\lambda = 0.71073$ Å.
[b] $R(F) = \Sigma||F_o|-|F_c||/\Sigma|F_o|$ for $F_o^2 > 2\sigma(F_o^2)$.
[c] For $F_o^2 < 0$, $w^{-1} = \sigma^2(F_o^2)$; for $F_o^2 \geq 0$, $w^{-1} = \sigma^2(F_o^2)+(0.0501\times P)^2+33.397\times P$ ($[Hg_3Te_2][UCl_6]$); $w^{-1} = \sigma^2(F_o^2)+(0.0197\times P)^2+133.94\times P$ ($[Hg_4As_2][UCl_6]$); $P = (F_o^2+2\times F_c^2)/3$.

Table 2
Selected interatomic distances (Å) and angles (deg) for $[Hg_3Te_2][UCl_6]$[a]

U–Cl(1) × 2	2.622(3)
U–Cl(2) × 2	2.623(3)
U–Cl(3) × 2	2.624(3)
Hg(1)–Te	2.664(1)
Hg(1)–Te	2.666(1)
Hg(2)–Te × 2	2.672(1)
Cl–U–Cl	180
Cl(1)–U–Cl(2) × 2	88.20(10)
Cl(1)–U–Cl(3) × 2	88.35(10)
Cl(2)–U–Cl(3) × 2	89.06(10)
Te–Hg(1)–Te	172.82(2)
Te–Hg(2)–Te	180
Hg(1)–Te–Hg(1)	95.48(3)
Hg(1)–Te–Hg(2)	94.64(3)
Hg(1)–Te–Hg(2)	96.35(3)

[a] U and Hg(2) have crystallographic site symmetry $\bar{1}$.

Table 3
Selected interatomic distances (Å) and angles (deg) for $[Hg_4As_2][UCl_6]$

U–Cl(1)	2.605(3)	Cl(2)–U–Cl(6)	86.4(1)
U–Cl(2)	2.620(3)	Cl(3)–U–Cl(4)	92.1(1)
U–Cl(3)	2.624(3)	Cl(3)–U–Cl(5)	93.1(1)
U–Cl(4)	2.625(3)	Cl(3)–U–Cl(6)	90.1(1)
U–Cl(5)	2.629(3)	Cl(4)–U–Cl(5)	90.5(1)
U–Cl(6)	2.639(3)	Cl(4)–U–Cl(6)	177.8(1)
Hg(1)–As(1)	2.480(1)	Cl(5)–U–Cl(6)	89.8(1)
Hg(1)–As(2)	2.480(1)	As(1)–Hg(1)–As(2)	161.51(4)
Hg(2)–As(1)	2.467(1)	As(1)–Hg(2)–As(2)	175.73(4)
Hg(2)–As(2)	2.469(1)	As(1)–Hg(3)–As(2)	175.67(4)
Hg(3)–As(1)	2.462(1)	As(1)–Hg(4)–As(2)	167.96(4)
Hg(3)–As(2)	2.464(1)	Hg(1)–As(1)–Hg(2)	118.98(5)
Hg(4)–As(1)	2.485(1)	Hg(1)–As(1)–Hg(3)	108.41(4)
Hg(4)–As(2)	2.481(1)	Hg(1)–As(1)–Hg(4)	103.59(4)
		Hg(2)–As(1)–Hg(3)	107.32(4)
Cl(1)–U–Cl(2)	90.2(1)	Hg(2)–As(1)–Hg(4)	111.66(5)
Cl(1)–U–Cl(3)	179.3(1)	Hg(3)–As(1)–Hg(4)	106.19(5)
Cl(1)–U–Cl(4)	88.6(1)	Hg(1)–As(2)–Hg(2)	117.86(5)
Cl(1)–U–Cl(5)	86.6(1)	Hg(1)–As(2)–Hg(3)	108.76(4)
Cl(1)–U–Cl(6)	89.3(1)	Hg(1)–As(2)–Hg(4)	106.91(4)
Cl(2)–U–Cl(3)	90.0(1)	Hg(2)–As(2)–Hg(3)	102.82(4)
Cl(2)–U–Cl(4)	93.2(1)	Hg(2)–As(2)–Hg(4)	106.57(4)
Cl(2)–U–Cl(5)	175.1(1)	Hg(3)–As(2)–Hg(4)	114.19(5)

2.6. Single-crystal optical measurements

Absorption measurements with polarized light were performed over the range from 400 nm (3.10 eV) to 900 nm (1.38 eV) at 293 K on single crystals of $[Hg_3Te_2][UCl_6]$ (green) and $[Hg_4As_2][UCl_6]$ (red) with the use of a Nikon TE300 inverted microscope coupled by fiber optics to an Ocean Optics model S2000 spectrometer. The procedure used has been described previously [23].

3. Results and discussion

3.1. Syntheses

Green single crystals of $[Hg_3Te_2][UCl_6]$ were obtained in 70 wt% yield by the stoichiometric reaction of UCl_4, $HgCl_2$, and HgTe at 1123 K. Larger single crystals were obtained by lowering the reaction temperature to 873 K, and increasing the reaction time from 96 to 120 h. Red single crystals of $[Hg_4As_2][UCl_6]$ were produced by the reaction of U, As, and Hg_2Cl_2 at 788 K in 80 wt% yield relative to U.

The compounds $[Hg_3Q_2][UCl_6]$ (Q = S, Se) were also obtained in crystalline form from the stoichiometric reactions of UCl_4, $HgCl_2$, and HgQ (Q = S, Se) at 1123 K. Twinning and absorption problems (owing to irregular crystal shapes) resulted in poor structure determinations. The unit-cell constants—$[Hg_3S_2][UCl_6]$: $a = 6.865(5)$ Å, $b = 7.368(5)$ Å, $c = 13.143(8)$ Å, $\beta = 91.339(8)^\circ$; $[Hg_3Se_2][UCl_6]$: $a = 6.830(1)$ Å, $b = 7.520(2)$ Å, $c = 13.300(3)$ Å, $\beta = 91.88(3)^\circ$—and the structure refinements, however, show unequivocally that these compounds are isostructural with $[Hg_3Te_2][UCl_6]$.

Attempts to synthesize analogues with different halides or pnictides proved unsuccessful. The reaction of UBr_4, Hg_2Br_2, and HgTe to produce $[Hg_3Te_2][UBr_6]$ resulted only in the recrystallization of UBr_4. The stoichiometric reaction of UI_4, HgI_2, and HgTe to produce $[Hg_3Te_2][UI_6]$ yielded the known ternary mercury iodochalcogenide $Hg_3Te_2I_2$ [24]. Attempted syntheses of the phosphorus or antimony variants of $[Hg_4As_2][UCl_6]$, with the use of the same procedure but with elemental red P or Sb in place of As, also failed.

3.2. Structures

$[Hg_3Te_2][UCl_6]$ is isostructural with the known compounds $[Hg_3Q_2][MX_6]$ (Q = S, Se; M = Zr, Hf; X = Cl, Br) [7]. The structure of $[Hg_3Te_2][UCl_6]$ is shown in Fig. 1. It comprises $^2_\infty[Hg_3Te_2^{2+}]$ layers perpendicular to a^* that form Hg_6Te_6 rings. The Hg atoms are two-coordinate, with a linear geometry. The Te atoms are three-coordinate, with a trigonal pyramidal geometry. The Hg_6Te_6 rings adopt the chair conformation (Fig. 2), as is seen in organic molecules such as cyclohexane. Located between the $^2_\infty[Hg_3Te_2^{2+}]$ layers are discrete $[UCl_6]^{2-}$ octahedra.

The $[Hg_3Q_2^{2+}]$ moiety is known to form various structural motifs with one-, two-, or three-dimensional character. β-$Hg_3S_2Br_2$ [25] has $^1_\infty[Hg_3S_2^{2+}]$ zigzag chains in the [100] direction, with Br atoms in the loops of each chain and between adjacent chains. $[Hg_3Se_2][Se_2O_5]$ exhibits $^1_\infty[Hg_3Se_2^{2+}]$ stair-like chains in the [010] direction. The compound α-$Hg_3S_2Cl_2$ [26] contains $[Hg_3S_2^{2+}]$ chains that extend in three directions.

The well-known hexachlorouranate(IV) octahedral anion $[UCl_6]^{2-}$ has been crystallized with a variety of countercations, including $[N(CH_3)_4]^+$ [27], $[P(C_6H_5)_3(C_2H_5)]^+$ [28], 1-butyl-3-methyl-imidazolium [29], and $[UCl_2((CH_3)_2SO)_6]^{2+}$ [30]. However, until the present discovery of $[Hg_3Te_2][UCl_6]$ and $[Hg_4As_2][UCl_6]$, no purely inorganic structure had contained the discrete $[UCl_6]^{2-}$ anion. The most closely related compounds are the alkali-metal uranium chlorides, A_2UCl_6 (A = Li, Na, Cs) [31,32], but in these structures there are some $A\cdots$CL interactions.

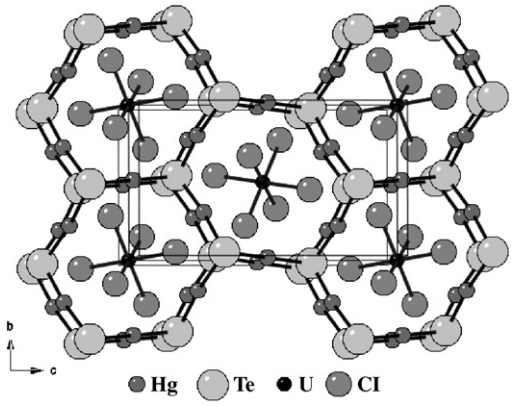

Fig. 1. The structure of $[Hg_3Te_2][UCl_6]$ viewed down a^*.

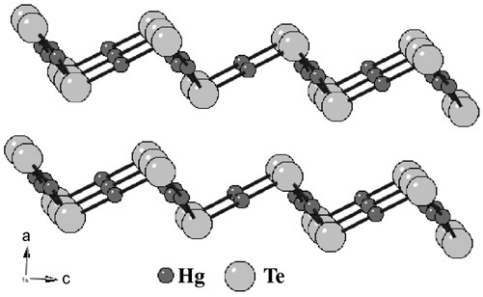

Fig. 2. Chair conformation of the Hg_6Te_6 rings in $[Hg_3Te_2][UCl_6]$ viewed down [010].

For $[Hg_3Te_2][UCl_6]$, the formal oxidation states may be assigned as +4, +2, −2, and −1 for U, Hg, Te, and Cl, respectively. The interatomic distances listed in Table 2 are normal. The following comparisons can be made: U–Cl, 2.622(3)–2.624(3) Å vs. 2.621(7) Å in Cs_2UCl_6 [32]; Hg–Te, 2.664(1)–2.672(1) Å vs. 2.644 Å in $Hg_3Te_2Cl_2$ [26].

Although many types of mercury–arsenic frameworks are known in the literature, $[Hg_4As_2][UCl_6]$ appears to be a new structure type. Its structure is shown in Fig. 3. All the Hg atoms are two-coordinate, with a linear geometry. The structure contains $^2_\infty[Hg_3As_2]$ layers along [010] that form Hg_6As_6 rings. These adopt the twist-boat conformation, in contrast to the chair conformation of the Hg_6Te_6 rings in $[Hg_3Te_2][UCl_6]$. Unlike the Te atoms in $[Hg_3Te_2][UCl_6]$, which are three-coordinate, the As atoms are four-coordinate with a distorted tetrahedral geometry. The As atoms in each layer of the Hg_6As_6 rings are connected by a Hg atom; this results in a three-dimensional framework (Fig. 4). The Hg atoms that link neighboring $^2_\infty[Hg_3As_2]$ layers result in the formation of steps, as shown in Fig. 5. These steps contain repeat segments of Hg_8As_8 octagons, Hg_6As_6 hexagons, and Hg_4As_4 squares, all with distorted geometries. Located between the $^2_\infty[Hg_3As_2]$ layers are discrete $[UCl_6]^{2-}$ octahedra.

$[Hg_4As_2][UCl_6]$ is the first known example of the $[Hg_4As_2]$ structural moiety. Previous compounds have most commonly contained the $[Hg_6As_4]$ moiety, but other known structural fragments include $[Hg_7As_4]$, $[HgAs_2]$, $[Hg_3As_2]$, $[Hg_{11}As_4]$, $[Hg_{23}As_{12}]$, and $[Hg_{13}As_8]$. All examples of the $[Hg_6As_4]$ structural moiety contain As–As bonding in the form of As_2^{4-} dumbbells. This results in cavities of two different sizes within the cationic

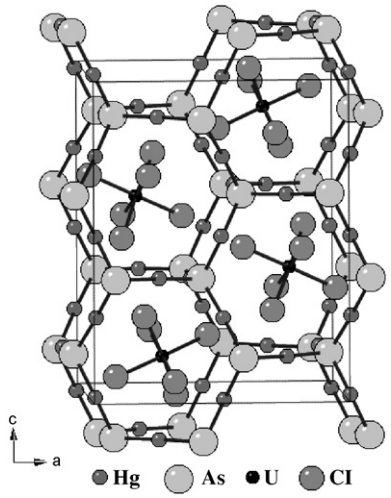

Fig. 3. The structure of $[Hg_4As_2][UCl_6]$ viewed down [010].

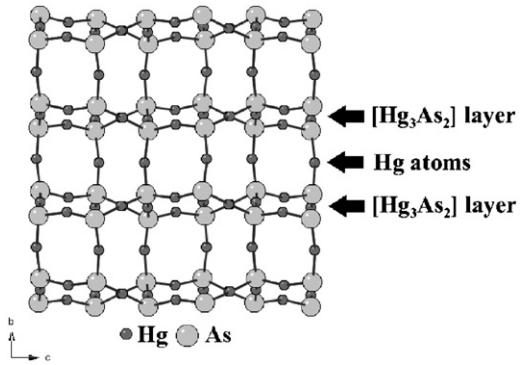

Fig. 4. Multiple $[Hg_3As_2]$ layers interconnected by Hg atoms. View is down [100].

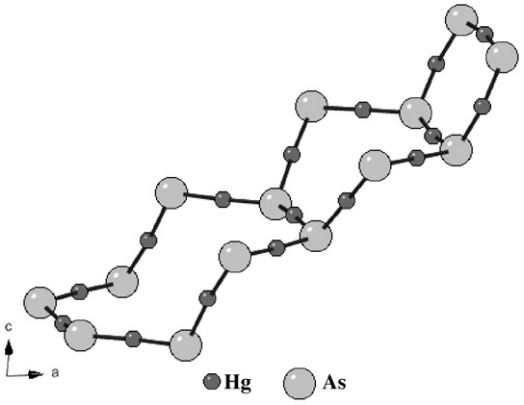

Fig. 5. The steps in $[Hg_4As_2][UCl_6]$ containing repeated units of Hg_8As_8 octagons, Hg_6As_6 hexagons, and Hg_4As_4 squares, all with distorted geometries.

framework. In most cases, such as $[Hg_6As_4][TiCl_6]Cl$ [10], one cavity is occupied by a metal of oxidation state +3. This metal is coordinated by six halogen atoms to form an octahedral $[MX_6]^{3-}$ anion. To balance the 4+ charge of the $[Hg_6As_4]$ moiety, the other cavity is filled by a lone halogen anion. Less common is the example of $[Hg_6As_4][FeBr_6]Hg_{0.6}$ [33], in which the Fe atom has an oxidation state of +2, so the charges of the cation and anion are already balanced. The second cavity is partially filled by zerovalent mercury atoms. $[Hg_6As_4][AgCl_3]_2$ [34] has a different arrangement in which the cavities are filled by an infinite chain of corner-sharing $[AgCl_3]^-$ tetrahedral anions. Both the $[Hg_7As_4]$ [11] and $[Hg_3As_2]$ [12] moieties also contain As_2^{4-} dumbbells, but in structures containing these species the cavities in the framework are of equal size. There is no As–As bonding in the $[Hg_{11}As_4]^{4+}$ cation of $[Hg_{11}As_4][GaBr_4]_4$ [14] so all As atoms may be assigned an oxidation state of −3. Rather, there are $^2_\infty[Hg_6As_4]$ layers with Hg_6As_6 rings that are interconnected in the [001] direction alternately by Hg_2^{2+} and Hg_3^{2+} units. The $[Hg_{23}As_{12}]$ [35] moiety contains one As_2^{4-} dumbbell per 12 As atoms and has equivalent cavities. The $[Hg_{13}As_8]$ [35] moiety contains three As_2^{4-} dumbbells per eight As atoms, and has nonequivalent cavities. The $[Hg_2As]$ motif in $[Hg_2As]_2[CdI_4]$ [15] is structurally the most similar to that in the present $[Hg_4As_2][UCl_6]$ structure. Neither compound has As–As nor Hg–Hg bonding, and all cavities are identical. The key difference is that $[Hg_2As]_2[CdI_4]$ (space group $P2_1$) has tetrahedral anions in the cavities, whereas $[Hg_4As_2][UCl_6]$ (space group $P2_1/c$) has octahedral anions in the cavities.

For $[Hg_4As_2][UCl_6]$, the formal oxidation states may be assigned as +4, +2, −3, and −1 for U, Hg, As, and Cl, respectively. The interatomic distances listed in Table 3 are normal. The following comparisons can be made: U–Cl, 2.605(3)–2.639(3) Å vs. 2.621(7) Å in Cs_2UCl_6 [32]; Hg–As, 2.462(1)–2.480(1) Å vs. 2.491(1)–2.494(1) Å in $[Hg_6As_4][TiCl_6]Cl$ [10].

Although the mercury chalcohalides contain mercury-chalcogen cationic moieties, there are also numerous examples of mercury-chalcogen anionic moieties. Ternary compounds with an alkali metal or alkaline-earth metal, mercury, and a chalcogen contain mercury-chalcogen anionic structural motifs separated by discrete alkali cations or alkaline-earth cations. The compounds $Na_2Hg_3S_4$ [36] and $Rb_2[Hg_3Te_4]$ [37] feature $^2_\infty[Hg_3Q_4^{2-}]$ layers with Na^+ or Rb^+ cations between the layers. As another example, the compound $Rb_4[Hg_5(Te_2)_2(Te_3)_2Te_3]$ [38] possesses $^1_\infty[Hg_5(Te_2)_2(Te_3)_2Te_3^{4-}]$ ribbons in the [010] direction separated by Rb^+ cations.

Similarly, there are also some examples of mercury-pnictogen anionic moieties. Ternary compounds of an alkali metal, mercury, and a pnictogen (such as As) contain mercury-pnictogen anionic structural motifs with alkali metal countercations. The compound KHgAs [39] features $^2_\infty[HgAs^-]$ sheets of Hg_3As_3 hexagons, with K^+ cations between the layers. Another example, $K_4[HgAs_2]$ [40], contains discrete linear $[As–Hg–As]^{4-}$ anions separated by K^+ cations.

3.3. Magnetic susceptibility

$[Hg_3Te_2][UCl_6]$ exhibits a small magnetic susceptibility, which is essentially independent of temperature between 60 and 400 K. The average temperature-independent magnetic susceptibility over the range 60–320 K is $25.4(4)\times10^{-4}$ emu/mol. This is similar to the average temperature-independent magnetic susceptibilities for other compounds containing the $[UCl_6]^{2-}$ anion, such as $20.5(3)\times10^{-4}$ emu/mol for $[PBuPh_3]_2[UCl_6]$ [41], 22.43×10^{-4} emu/mol for $[N(CH_3)_4]_2[UCl_6]$ [42], and 24.4×10^{-4} emu/mol for Cs_2UCl_6 [43].

The temperature-independent magnetic susceptibility of hexachlorouranate(IV) compounds has been explained [44] on the basis of the perturbation of the ground-state electronic configuration. U^{4+} exhibits an f^2 ground-state electronic configuration, with an $^3H_4$ ground state for the free ion. Placing a U^{4+} ion at the body center of an octahedral configuration of six negative point charges (Cl^- ligands) results in four symmetry representations (Γ_1, Γ_3, Γ_4, and Γ_5). The singlet state, Γ_1, is lowest in energy. The magnetic susceptibility will not be affected by the Γ_3 and Γ_5 states because they are not mixed with Γ_1 by the magnetic field.

Therefore, the temperature-independent paramagnetism is due solely to the ground Γ_1 state and the Γ_4 state lying ΔE above it. From tabulated values for the electronic levels, the temperature-independent molar susceptibility for the $[UCl_6]^{2-}$ anion in Cs_2UCl_6 has been calculated [45] to be 26.7×10^{-4} emu/mol, which agrees very well with the value of $25.4(4) \times 10^{-4}$ emu/mol obtained here for $[Hg_3Te_2][UCl_6]$.

3.4. Optical properties

The broad absorbance spectrum for $[Hg_3Te_2][UCl_6]$ exhibits some intense absorption bands at 1.59, 1.84, 1.93, and 2.05 eV whereas that for $[Hg_4As_2][UCl_6]$ exhibits peaks at 1.58, 1.87, and 1.93 eV (Supporting material). These absorbance peaks are characteristic of *f–f* optical transitions, and the values correspond well with those observed in other compounds with the $[UCl_6]^{2-}$ anion, including Cs_2UCl_6, $[N(CH_3)_4]_2[UCl_6]$, and $[N(C_2H_5)_4]_2[UCl_6]$ [46,47]. Other compounds with uranium in the +4 oxidation state, such as KU_2Se_6 [48] and RbU_2SbS_8 [49], also display *f–f* optical transitions in their absorbance spectra.

The band gaps for these compounds could not be determined precisely because the absorption edges are obscured by interference from the *f–f* optical transitions. However, a rough approximation from the spectra places the band gaps of $[Hg_3Te_2][UCl_6]$ and $[Hg_4As_2][UCl_6]$ around 2.6 and 1.9 eV, respectively. A band gap of 2.6 eV for $[Hg_3Te_2][UCl_6]$ is consistent with the light-green color of the compound, and also with the band gap of 2.63 eV determined for $[Hg_3Se_2][Se_2O_5]$ [8]. A band gap of 1.9 eV for $[Hg_4As_2][UCl_6]$ is consistent with the red color of the compound, and also corresponds to the band gaps found by diffuse reflectance spectroscopy for some similar compounds: 2.05 eV for $[Hg_6As_4][CdCl_6]Hg_{0.5}$, 2.01 eV for $[Hg_6As_4][HgCl_6]Hg_{0.5}$, and 1.94 eV for $[Hg_6As_4][CdBr_6]$ [50].

Supporting material

The absorbance spectra and the crystallographic files in CIF format for $[Hg_3Te_2][UCl_6]$ and $[Hg_4As_2][UCl_6]$. These latter files have been deposited with FIZ Karlsruhe as CSD numbers 419437 and 419438, respectively. These data may be obtained free of charge by contacting FIZ Karlsruhe at +497247808 666 (fax) or crysdata@fiz-karlsruhe.de (e-mail).

Acknowledgments

We thank Dr. George H. Chan and Prof. Richard P. Van Duyne for help with the use of their single-crystal absorption spectrometer. This research was supported by the US Department of Energy BES Grant ER-15522.

References

[1] J.A. Cody, M.F. Mansuetto, M.A. Pell, S. Chien, J.A. Ibers, J. Alloys Compd. 219 (1995) 59–62.
[2] A. Daoudi, H. Noël, J. Alloys Compd. 233 (1996) 169–173.
[3] A.V. Tkachuk, C.P.T. Muirhead, A. Mar, J. Alloys Compd. 418 (2006) 39–44.
[4] J.A. Morkowski, A. Szajek, E. Talik, R. Troc, J. Alloys Compd. 443 (2007) 20–25.
[5] M.E. Kassner, D.E. Peterson, Phase Diagrams of Binary Actinide Alloys, ASM International, Materials Park, 1995.
[6] H. Puff, G. Lorbacher, D. Heine, Naturwissenschaften 56 (1969) 461.
[7] J. Beck, S. Hedderich, J. Solid State Chem. 172 (2003) 12–16.
[8] J.-P. Zou, G.-C. Guo, S.-P. Guo, Y.-B. Lu, K.-J. Wu, M.-S. Wang, J.-S. Huang, Dalton Trans. 42 (2007) 4854–4858.
[9] A.V. Olenev, A.V. Shevelkov, J. Solid State Chem. 160 (2001) 88–92.
[10] J. Beck, U. Neisel, Z. Anorg. Allg. Chem. 626 (2000) 1620–1626.
[11] A.V. Olenev, A.I. Baranov, O.S. Oleneva, I.I. Vorontsov, M.Y. Antipin, A.V. Shevelkov, Eur. J. Inorg. Chem. 6 (2003) 1053–1057.
[12] J. Beck, U. Neisel, Z. Anorg. Allg. Chem. 627 (2001) 2016–2022.
[13] A.V. Olenev, T.A. Shestimerova, W. Schnelle, A.V. Shevelkov, Z. Anorg. Allg. Chem. 631 (2005) 1698–1701.
[14] A.V. Olenev, A.V. Shevelkov, Angew. Chem., Int. Ed. Engl. 40 (2001) 2353–2354.
[15] J.-P. Zou, D.-S. Wu, S.-P. Huang, J. Zhu, G.-C. Guo, J.-S. Huang, J. Solid State Chem. 180 (2007) 805–811.
[16] J.A. Hermann, J.F. Suttle, Uranium(IV) chloride, in: T. Moeller (Ed.), Inorganic Synthesis, vol. 5, McGraw-Hill Book Company, New York, 1957, pp. 143–145.
[17] A.J.K. Haneveld, F. Jellinek, J. Less-Common Met. 18 (1969) 123–129.
[18] Bruker, SMART Version 5.054 Data Collection and SAINT-Plus Version 6.45a Data Processing Software for the SMART System, Bruker Analytical X-ray Instruments, Inc., Madison, WI, USA, 2003.
[19] Bruker, APEX2 Version 2.1-4, Bruker Analytical X-ray Instruments, Inc., Madison, WI, USA, 2006.
[20] G.M. Sheldrick, Acta Crystallogr. Sect. A: Found. Crystallogr. 64 (2008) 112–122.
[21] L.M. Gelato, E. Parthé, J. Appl. Crystallogr. 20 (1987) 139–143.
[22] L.N. Mulay, E.A. Boudreaux, Theory and Applications of Molecular Diamagnetism, Wiley-Interscience, New York, 1976.
[23] K. Mitchell, F.Q. Huang, E.N. Caspi, A.D. McFarland, C.L. Haynes, R.C. Somers, J.D. Jorgensen, R.P. Van Duyne, J.A. Ibers, Inorg. Chem. 43 (2004) 1082–1089.
[24] V.A. Lyakhovitskaya, N.I. Sorokina, A.A. Safonov, I.A. Verin, V.I. Andrianov, Kristallografiya 34 (1989) 835–838.
[25] Y.V. Voroshilov, V.A. Khudolii, V.V. Pan'ko, Y.V. Minets, Inorg. Mater. (Transl. Neorg. Mater.) 32 (1996) 1281–1286.
[26] H. Puff, J. Küster, Naturwissenschaften 49 (1962) 464–465.
[27] H.D. Hardt, E. Hofer, Naturwissenschaften 56 (1969) 88.
[28] M.R. Caira, J.F. de Wet, J.G.H. du Preez, B.J. Gellatly, Acta Crystallogr. Sect. B: Struct. Crystallogr. Cryst. Chem. 34 (1978) 1116–1120.
[29] S.I. Nikitenko, C. Hennig, M.S. Grigoriev, C. Le Naour, C. Cannes, D. Trubert, E. Bossé, C. Berthon, P. Moisy, Polyhedron 26 (2007) 3136–3142.
[30] G. Bombieri, K.W. Bagnall, J. Chem. Soc., Chem. Commun. 6 (1975) 188–189.
[31] P.J. Bendall, A.N. Fitch, B.E.F. Fender, J. Appl. Crystallogr. 16 (1983) 164–170.
[32] T. Schleid, G. Meyer, L.R. Morss, J. Less-Common Met. 132 (1987) 69–77.
[33] A.V. Olenev, O.S. Oleneva, M. Lindsjö, L.A. Kloo, A.V. Shevelkov, Chem. Eur. J. 9 (2003) 3201–3208.
[34] O.S. Oleneva, A.V. Olenev, E.V. Dikarev, A.V. Shevelkov, Eur. J. Inorg. Chem. 20 (2004) 4006–4010.
[35] A.V. Olenev, A.V. Shevel'kov, B.A. Popovkin, Russ. J. Inorg. Chem. (Transl. Zh. Neorg. Khim.) 44 (1999) 1853–1861.
[36] K.O. Klepp, J. Alloys Compd. 182 (1992) 281–288.
[37] J. Li, Z. Chen, K.-C. Lam, S. Mulley, D.M. Proserpio, Inorg. Chem. 36 (1997) 684–687.
[38] X. Chen, X. Huang, J. Li, Inorg. Chem. 40 (2001) 1341–1346.
[39] R. Vogel, H.-U. Schuster, Z. Naturforsch. B: Anorg. Chem. Org. Chem. 35 (1980) 114–116.
[40] M. Asbrand, B. Eisenmann, M. Somer, Z. Kristallogr. New Cryst. Struct. 212 (1997) 79.
[41] J.P. Day, L.M. Venanzi, J. Chem. Soc. A 2 (1966) 197–200.
[42] G.A. Candela, C.A. Hutchison Jr., W.B. Lewis, J. Chem. Phys. 30 (1959) 246–250.
[43] B.N. Figgis, D.J. Mackey, Aust. J. Chem. 27 (1974) 2053–2055.
[44] C.A. Hutchison Jr., G.A. Candela, J. Chem. Phys. 27 (1957) 707–710.
[45] R.A. Satten, C.L. Schreiber, E.Y. Wong, J. Chem. Phys. 42 (1965) 162–171.
[46] R.A. Satten, D. Young, D.M. Gruen, J. Chem. Phys. 33 (1960) 1140–1151.
[47] S.A. Pollack, R.A. Satten, J. Chem. Phys. 36 (1962) 804–816.
[48] H. Mizoguchi, D. Gray, F.Q. Huang, J.A. Ibers, Inorg. Chem. 45 (2006) 3307–3311.
[49] K.-S. Choi, M.G. Kanatzidis, Chem. Mater. 11 (1999) 2613–2618.
[50] J.-P. Zou, Y. Li, M.-L. Fu, G.-C. Guo, G. Xu, X.-H. Liu, W.-W. Zhou, J.-S. Huang, Eur. J. Inorg. Chem. 7 (2007) 977–984.